Energy 204 (2020) 117929

Contents lists available at ScienceDirect

Energy

journal homepage: www.elsevier.com/locate/energy

Optimal scheduling of electric vehicles car-sharing service with multi-temporal and multi-task operation

Kexing Lai [a], Tao Chen [b, *], Balasubramaniam Natarajan [a]

[a] Department of Electrical and Computer Engineering, Kansas State University, Manhattan, KS, 66506, USA
[b] School of Electrical Engineering, Southeast University, Nanjing, 210000, China

ARTICLE INFO

Article history:
Received 27 January 2020
Received in revised form
4 May 2020
Accepted 20 May 2020
Available online 30 May 2020

Keywords:
Car-sharing
Electric vehicle
Optimal routing and charging
Time-of-use price

ABSTRACT

The booming car-sharing industry and gig economy embody the critical need for enhancing utilization of vehicular resources. For this emerging business paradigm, the scheduling optimization considering interdependent scenarios and constraints becomes the key issue. In addition, telecommuting jobs are becoming increasingly popular with the support of highly developed telecommunication technologies. This paper develops a framework for optimal scheduling of an electric vehicle owner, who seeks to share the vehicle in a cost-effective manner while ensure sufficient working hours on a telecommuting job at home. The electric vehicle owner aims at minimizing delivery times of customers and charging cost simultaneously, considering a time-of-use charging pricing mechanism, while satisfying customers demands and working hour requirements. To describe this optimal scheduling problem, this paper firstly introduces three elements: *state*, *action* and *task*. Specifically, three states are involved, including charging state, parking state and transporting state. Further, actions of electric vehicle owner are used as the links for state transitions. Finally, multiple tasks are completed sequentially in a multi-temporal time horizon, where each task is assigned with a selected state. The proposed model formulates the scheduling problem for each state. Moreover, supplementary constraints representing state transitions, working hour requirement and energy neutral position of an electric vehicle battery are further incorporated to establish the optimal scheduling model for the entire process. This paper presents the first-of-its-kind work incorporating all the vital aspects of a well-defined optimal scheduling problem, in which an electric vehicle owner seeks car-sharing opportunity and conducts a telecommuting job at home, considering multiple states, actions and tasks in a continuous multi-temporal horizon. The numerical studies demonstrate the effectiveness of the designed framework in terms of optimizing routing selections and charging time allocation. The performance of the proposed model is also compared with baseline scenarios, and it finds that up to 18.5% cost saving can be accomplished by adopting the proposed model, which validates its cost benefits.

1. Introduction

Nowadays, the technology advances in both power energy industry and automotive industry promote the integration of the transportation electrification with modern smart city development [1]. With support of the ubiquitous presence of electric vehicles (EVs) and electric vehicle service equipment in many urbanized cities, this trend is even further catalyzed by internet-of-things (IoT) and smartphone communication technologies [2]. Additionally, with massive deployments of IoT communication devices distributed in smart cities, many new business models are also becoming possible to facilitate a new paradigm of transport service that shifts EV ownership to intelligent EV sharing. Successful multinational car-sharing companies (e.g. Uber, Lyft, DiDi) have significantly shaped transport service models with a considerable societal impact based on gig economy. It is believed that if the developments of EV car-sharing business models and operations of relevant energy infrastructures can be properly integrated, the entire society will in return benefit more from the technology-driven smart city development [3].

One of the unique features of EV sharing paradigm is customers' routing request demand can be linked and directed to certain

* Corresponding author.
E-mail addresses: klai@k-state.edu (K. Lai), taoc@seu.edu.cn (T. Chen), USAbala@ksu.edu (B. Natarajan).

https://doi.org/10.1016/j.energy.2020.117929
0360-5442/

energy demand portfolios of geographically distributed energy infrastructures [4]. As a result, the decision-making of EV routing and scheduling strategies should consider a variety of aspects including economic benefit (e.g., driving cost [5]), customer satisfaction (e.g., shortest path [6]), and even technical merit (e.g., voltage support [7]) for social welfare maximization. In contrast to the conventional vehicle routing problem (VRP), the EV car-sharing problem is usually more dynamic and can be modeled as an optimal routing and charging problem at the same time, with the consideration of various customers requests of pick-up and drop-off locations, besides starting points and final destinations [6].

In the prior publications in energy research field, EVs are usually modeled as lumped traffic flow characterized as charging demand mobility to the nearest regional charging station without detailed routing path selection [8,9]. For instance, in Ref. [10], the navigation of EVs with range anxiety is abstracted as stochastic driving behavior towards their pass-by charging service points. The queuing theory is often used to model the charging and waiting time requirements [10], which mainly focus on the charging station operation with emphasis on the distribution network mapping relationship rather than transport network. Some recent studies have also proposed co-simulation of power system and transport system, combining the studies of EV traffic flow and power flow [11,12]. However, the research focus of power grid service still dominates the focus of transport service in most relevant energy field studies. For example, the work in Ref. [13] considers a state representation of autonomous EVs and overall charging/driving behavior, but with the objective of providing operating reserve for power grid service. The routing problem of specific EV's driving behavior is neglected, like many other works [9,12]. In contrast to Ref. [13], the proposed model in this paper aims at maximizing EV owners' benefits with detailed routine selection strategy, along with price-responsive charging scheduling. Admittedly, some recent works [5,14,15] have begun to advocate the concept of electric vehicle routing problem (E-VRP), which studies the EV in-the-middle way charging behavior, along with its impact on the route selections in realistic transport networks. For instance, the work in Ref. [15] uses a two-phase heuristic method to solve an E-VRP with energy consumption uncertainty, considering the geographic space of a real transport network. Similar ideas can also be found in Ref. [16–18], which turned the spotlight on the E-VRPs coupled with the consideration of energy consumption. In Ref. [16], the work tackles the E-VRP with a nonlinear charging function and propose three new algorithms to identify the optimal charging decisions for a given route [17]. proposes an EV route selection and charging navigation optimization model, aiming to reduce EV users' travel costs and alleviate the load level of distribution systems [18]. incorporates a detailed model of topography, speed, acceleration and powertrain efficiency into the E-VRP. However, car-sharing models with customers requirements of pickup time windows are not covered in most of these works. Even a few papers integrate the EV optimal routing and charging problems, using a pick-up and delivery model [6,19], these proposed models are limited within a single task cycle. In other words, multi-temporal and multi-task operations, along with inter-temporal transitions are neglected. These over-simplified assumptions significantly limit their applications in the real world.

In this paper, we propose a new EV sharing service model, from an EV owner's perspective, which incorporates optimal routing and price-responsive charging schemes in a continuous multi-temporal horizon. This new service model is especially suitable for those EV owners who have telecommuting jobs, a. k.a. working from home jobs, which are becoming increasingly popular in most metropolis areas. This EV car-sharing model considers multi-temporal and multi-task operation, along with various inter-temporal constraints (e.g., multiple SoC cycles, several rounds of customer assignments) and variable charging price signals (e.g., time-of-use). Furthermore, for the proposed car-sharing service model, customers itineraries are determined beforehand, which means pickup locations and time windows, along with drop-off locations, are known to the EV owner. In this regard, customers choose to schedule their itineraries in advance to circumvent uncertainties of real-time car-sharing scheduling. Besides, compared to car-sharing platforms for real-time scheduling, this service model leads to a more cost-effective solution since the knowledge of customers itineraries would aid the driver in optimizing schedule in advance. This service model is considered as suitable for customers, who reside in areas with insufficient real-time carpool resources, to commute efficiently with lower cost. On the other hand, even in areas with redundant real-time car-sharing resources, this model can be adopted as an effective and efficient complimentary scheme for satisfying the diversity of customers' demands and preferences. In the real world, Scoop, a company with over 100,000 users and a collective 2 million carpool trips till October 2017, has adopted a similar service model that requires customers itineraries at least 9 h in advance [20,21].

To summarize, this work addresses the research gap of lacking a comprehensive optimization model that captures all the vital aspects of EV sharing service scheduling, including multi-temporal and multi-task operation, time-varying charging price and quality of service. This work lays the groundwork for developing relevant real-world business paradigms, which would further promote car sharing incentive for EV owners conducting telecommuting jobs.

Finally, the contributions of this paper can be summarized as follows:

1. An EV car-sharing model is proposed on top of conventional vehicle routing problems, which considers customers pick-up and drop-off requirements in addition to optimal EV routing and charging behaviors. Additionally, the multi-temporal multi-task operation, instead of simple one-task assignment within a single time cycle, is studied. Interrelationship between different tasks, time slots and state transition constraints are also considered.
2. The optimization model enables decision-making over multiple time slots and consideration of time-of-use electricity price information in energy infrastructure. In particular, the numerical studies show that charging price signals impose significant impacts on the selection of delivering routines and charging behavior.
3. The EV car-sharing model is tested and validated in various application scenarios. The effects of different hyper-parameters or factors on system performance are studied. The ultimate cost benefit is justified by up to 18.5% cost saving via adopting the proposed model. Moreover, the reformulation effort of recasting the original optimization model into a mixed-integer linear programming (MILP) problem is demonstrated to be valuable as using heuristic solution techniques to solve the original problem results in considerably worse outcomes.

2. Problem description and assumption

2.1. Problem description

The fundamental component of this study is the decision-making process of an EV owner, who has the desire of sharing of vehicular resource, meanwhile conducting a telecommuting job at home. The objective of the EV owner's optimal scheduling is to minimize charging cost and delivery times of customers, while

satisfy customers requests and working hour requirements. This problem can be described by three elements, namely *state*, *action* and *task*.

Three states are involved for the EV's status: *charging state*, *parking state* and *transporting state*. In the charging state, the EV owner is working at home, while the EV is being charged. Similarly, the parking state refers to the fact that the EV owner is working at home with EV operated in idle non-charging mode. In the transporting state, the EV owner is in the process of delivering a customer with the pre-defined pickup time and location information, as well as the drop-off location information. Apart from state, the EV owner needs to determine the action taken after the ongoing state, including *go parking*, *go charging* and *go transporting* after the ongoing state. Finally, the EV owner needs to finish multiple tasks throughout the entire time horizon, during which a specific state should be selected for each task. In other words, as the *states* are independent of the process of time elapsing, *tasks* are introduced to bridge states and time evolution. Fig. 1 (a) presents state transitions from the perspective of the actions taken, which reflects the mapping relationship between actions and resulting states. In addition, Fig. 1(b) depicts a conceptual diagram representing the time evolving process of the entire horizon. As seen, the simulation evolves through multiple tasks, where a certain state is assigned for each task. For instance, parking state is assigned to task 1, which is conducted from 0:00 to 1:10. Sequentially, charging state is assigned to task 2, from 1:10 to 2:20, and transporting state is assigned to task 3 after that from 2:20 to 2:40. The course of time will continue till the end of horizon. Note that the time duration of each task often depends on the specific condition. For example, the time duration of a task assigned with transporting state depends on the customer's pickup and dropoff locations.

The proposed overall optimization framework for optimizing the EV owner can be visualized as Fig. 2. The objective function aims to minimize time consumption of delivering customers and charging cost with time-of-use charging price scheme. The constraints are composed by the state specified constraints and the supplementary constraints that define state transition conditions, working hour requirement and energy neutral position requirement of EV battery.

2.2. Assumptions

To simplify the formulation while maintain sufficiently precise representation of reality, the proposed optimization model is developed based on the following assumptions:

1. Customers itineraries are user-inputs and determined beforehand, which implies the fact that pickup locations and time windows, along with drop-off locations, are known to the EV owner.
2. The charging rate of EV battery is assumed to be fixed and vehicle-to-grid operation is not considered in this work.
3. Here, we assume that the EV owner is conducting a telecommuting work at home. Therefore, for transporting state, the starting and ending locations are designated at home to fulfill a certain work hour requirement. Besides, the home is equipped with a charging port and a parking lot for charging and parking states, respectively.

Note that this work presents an optimization model to determine EV car-sharing services scheduling considering multi-temporal and multi-task operation, which lays the groundwork for developing the relevant real-world business models. In practice, unexpected events and scenarios might lead to delays and incomplete service, which could be addressed by other mechanisms such as fine, bad rating, etc. The relevant discussion is out of scope here.

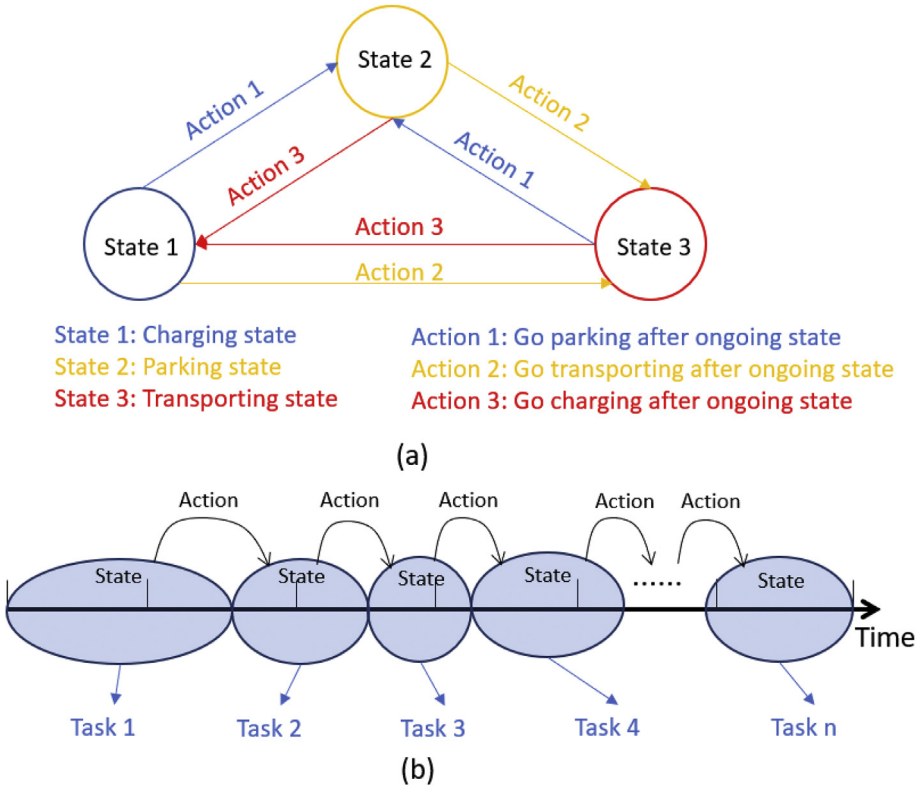

Fig. 1. Conceptual diagram for representing state transitions via, (a) actions, (b) tasks.

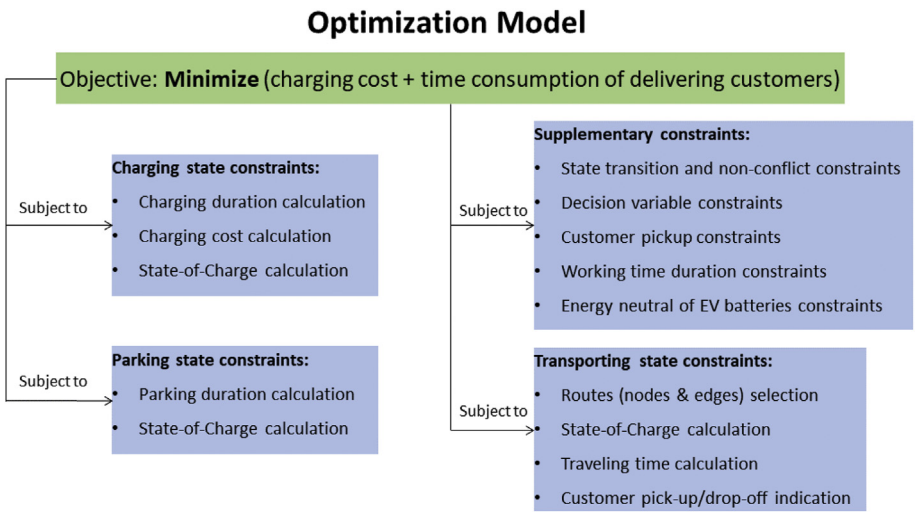

Fig. 2. Optimization model illustration for optimal EV scheduling and travel routing, including constraints of state and supplemental constraints.

3. Mathematical formulation

3.1. If-else statement

For this model, multiple $if-else$statements are required to configure multiple constraints. Here, we summarize all the involved types and reformulate them to constraints.

We define $if-else$statement I: "if condition is true, x = y; else, x and y are free variables", we use a binary variable b to indicate the true or false state ($b = 1$ means the condition is true, $b = 0$means otherwise). The constraint $-M(1-b) \le x - y \le M(1-b)$can precisely formulate this $if-else$statement, where M is a sufficiently large number.

We define $if-else$ statement II: "if condition is true, $x \ge (\le) y$; else, x and y are free variables", similarly, we use a binary variable b to indicate the true or false state ($b = 1$ means the condition is true, $b = 0$means otherwise). The constraint $x*b \ge (\le) y*b$ is equivalent to this $if-else$ statement.

Finally, we define $if-else$ statement III shown in (1), which can be exactly replaced by (2).

$$b = \begin{cases} 1, & if \quad x \ge y \\ 0, & if \quad x < y \end{cases} \tag{1}$$

$$-M*(1-b) \le x - y \le M*b \tag{2}$$

3.2. Optimization model

The objective function (3) aims at minimizing three terms, i.e. C_1, $C_2$and C_3, which cover charging cost and total delivery time of customers. The nomenclature and variable explanations are provided in Table 1 − 3.

The term C_1 provides the charging cost if the charging state is within a single time period of charging price change h, i.e. $S_a^{V,C} U_{a,h}^{B,min} U_{a,h}^{B,max} = 1$. In other words, the charging state ($S_a^{V,C}$) occurs when both the starting time ($U_{a,h}^{B,min}$) and ending time ($U_{a,h}^{B,max}$) of this state is within a single time period of charging price change h ($U_{a,h}^{B,min} U_{a,h}^{B,max} = 1$). When the condition holds true, the charging cost is computed as the product of charging rate (Q^C), charging price of the corresponding timer period (P_h) and charging duration ($T_a^{C,max} - T_a^{C,min}$).

Similarly, when the charging state occupies two charging periods (h and $h+1$), the charging cost is computed as C_2. Specifically, when the charging starts from one period till the subsequent period ($U_{a,h}^{B,min} U_{a,h+1}^{B,max} = 1$), the charging cost is computed by adding charging costs of the earlier period ($Q^C P_h (T_h^{H,max} - T_a^{C,min})$) and the later period ($Q^C P_{h+1} (T_a^{C,max} - T_h^{H,min})$). As seen, the charging cost of the earlier period is decided by charging rate (Q^C), charging price of the earlier timer period (P_h) and charging duration of the earlier time period that is defined as the gap between the charging starting time ($T_a^{C,min}$) and ending time of the earlier period h ($T_h^{H,max}$). Similarly, the charging cost of the later period is decided by charging rate (Q^C), charging price of the later timer period (P_{h+1}) and charging duration of the later time period that is defined as the gap between the charging ending time ($T_a^{C,max}$) and starting time of the later period $h+1$($T_{h+1}^{H,min}$).

Finally, the total delivery time of customers, denoted by C_3, is computed by multiplying total time duration of delivering customers ($S_a^{V,T} T_{a,c}^{DC}$) and assigned weighting factor (ω) based on the decision maker's preference.

3.2.1. The relevant constraints of charging state (state 1)

The relevant constraints of charging state are elaborated as follows.

$$\text{subject to}: -M\left(1 - S_a^{V,C}\right) \le SoC_a^{C,tmax} - \left(SoC_a^{C,tmin} + \frac{Q^C \eta}{E^{max}} T_a^{C,D}\right) \le M\left(1 - S_a^{V,C}\right), \quad \forall a \in \Phi^{EA} \tag{8}$$

$$-M\left(1 - S_a^{V,C}\right) \le T_a^{C,max} - \left(T_a^{C,min} + T_a^{C,D}\right) \le M\left(1 - S_a^{V,C}\right), \ \forall a \in \Phi^{EA} \tag{9}$$

$$SoC_a^{C,tmax} S_a^{V,C} \le SoC^{max} S_a^{V,C}, \quad \forall a \in \Phi^{EA} \tag{10}$$

Table 1
Nomenclature.

Sets and Indices	
a	index of EV tasks in set, Φ^{EA}
n	index of nodes of transportation network in set, Φ^{TN}
l	index of edges (roads) of transportation network in set, Φ^{TI}
c	index of customers in set, Φ^{C}
h	index of time period of charging price change in set, H
Ω^{HN}	Set of home node
Ω^{HU} / Ω^{HD}	Set of upstream/downstream edges of home node
$\Omega_c^{P,N}$ / $\Omega_c^{Q,N}$	Set of pickup/dropoff nodes for customer c
$\Omega_n^{U,L}$ / $\Omega_n^{D,L}$	Set of upstream/downstream edges of node n
$\Omega_l^{U,N}$ / $\Omega_l^{D,N}$	Set of upstream/downstream nodes of node l
Parameters	
P_h	Charging price of electric vehicle at time period h ($/kWh)
$T_h^{H,min}$/$T_h^{H,max}$	Minimum/Maximum time value of time period h (second)
T^{D}	Time duration for a single time period of charging price change (second)
$T_c^{C,min}$/$T_c^{C,max}$	Minimum/Maximum time value of time window of picking up customer c (second)
T^{max}	Maximum time value of the entire time horizon
$T^{W,min}$	Minimum working time duration
E_l	Energy consumption of edge/road l (kWh)
τ_l	Time consumption of edge/road l (second)
Q^{C}	Charging rate of EV battery (kW/minute)
η	Efficiency of EV battery
SoC^{min}/SoC^{max}	Minimum/Maximum State-of-Charge of EV battery
SoC^{ini}	Initial State-of-Charge of EV battery
E^{max}	Energy capacity of EV battery (kWh)
ω	Weighting factor of reducing delivery time of customers
M	Sufficiently large numberVariables
$S_a^{V,C}$	Binary variable for indicating charging state in task a; 1 means the electric vehicle is operated in charging state in task a, 0 means otherwise
$S_a^{V,P}$	Binary variable for indicating parking state in task a; 1 means the electric vehicle is operated in parking state in task a, 0 means otherwise
$S_a^{V,T}$	Binary variable for indicating transporting state in task a; 1 means the electric vehicle is operated in transporting state in task a, 0 means otherwise

$$SoC_a^{C,tmin} S_a^{V,C} \geq SoC^{min} S_a^{V,C}, \quad \forall a \in \Phi^{EA} \tag{11}$$

Constraint (8) implies that, during charging state ($S_a^{V,C}$), the gap between the initial and final *SoC*values depends on charging rate (Q^C), battery efficiency and capacity (η and E^{max}), along with duration of the state ($T_a^{C,D}$). Constraint (9) indicates the time evolution of charging state, meaning the time value at the end of charging state ($T_a^{C,max}$) is equal to the time value at the beginning of the state ($T_a^{C,min}$) plus the time duration ($T_a^{C,D}$). Constraints (10) and (11) enforce the *SoC* value bounds within charging state ($S_a^{V,C} = 1$). Note that these constraints are for charging state exclusively, hence *if* − *else*statements I and II presented in the earlier section are applied. For instance, the exploitation of *if* − *else*statement I in constraint (4) can be witnessed, as "if during charging state ($S_a^{V,C} = 1$), $SoC_a^{C,tmax} = \left(SoC_a^{C,tmin} + \frac{Q^C \eta}{E^{max}} T_a^{C,D}\right)$, otherwise, they are free variables". The same logic is applied to (5). Besides, constraint (6) is formulated based on the *if* − *else*statement II, as "if during charging state ($S_a^{V,C} = 1$), $SoC_a^{C,tmax} \leq SoC^{max}$, otherwise, they are free variables", which is also applied to constraint (7). These *if* − *else*statements and similar logic are frequently used to configure constraints in the following.

$$-M\left(1 - U_{a,h}^{L,min}\right) \leq \left(T_a^{C,min} - T_h^{H,min}\right) \leq M U_{a,h}^{L,min}, \quad \forall a \in \Phi^{EA}, h \in H \tag{12}$$

$$-M\left(1 - U_{a,h}^{E,min}\right) \leq \left(T_h^{H,max} - T_a^{C,min}\right) \leq M U_{a,h}^{E,min}, \ \forall a \in \Phi^{EA}, h \in H \tag{13}$$

$$U_{a,h}^{L,min} U_{a,h}^{E,min} = U_{a,h}^{B,min}, \quad \forall a \in \Phi^{EA}, h \in H \tag{14}$$

$$-M\left(1 - U_{a,h}^{L,max}\right) \leq \left(T_a^{C,max} - T_h^{H,min}\right) \leq M U_{a,h}^{L,max}, \ \forall a \in \Phi^{EA}, h \in H \tag{15}$$

$$-M\left(1 - U_{a,h}^{E,max}\right) \leq \left(T_h^{H,max} - T_a^{C,max}\right) \leq M U_{a,h}^{E,max}, \ \forall a \in \Phi^{EA}, h \in H \tag{16}$$

$$U_{a,h}^{L,max} U_{a,h}^{E,max} = U_{a,h}^{B,max}, \quad \forall a \in \Phi^{EA}, h \in H \tag{17}$$

Constraints (12)–(14) determine the time period that starting time of the charging state ($T_a^{C,min}$) is located. Obviously, when the starting time of charging state is within a certain time period, its value should be higher than the minimum time value ($T_h^{H,min}$), as indicated by $U_{a,h}^{L,min}$in constraint (12), and lower than maximum time value ($T_h^{H,max}$), as indicated by $U_{a,h}^{E,min}$ in constraint (13), of that period. The *if* − *else*statement III, as introduced in (1) and (2), is used in (12) and (13) to enforce those requirements. Further, constraint (14) defines the value of $U_{a,h}^{B,min}$, which indicates whether starting time is between $T_h^{H,min}$and $T_h^{H,max}$, i.e. within the time period h. Similarly, the value of $U_{a,h}^{B,max}$can indicate whether final

Table 2
Nomenclature (cont').

$D_a^{V,C}$	Binary variable for indicating "go charging" action after task a; 1 means the electric vehicle will go charging after task a, 0 means otherwise
$D_a^{V,P}$	Binary variable for indicating "go parking" action after task a, 1 means the electric vehicle will go parking after task a, 0 means otherwise
$D_a^{V,T}$	Binary variable for indicating "go transporting" action after task a; 1 means the electric vehicle will go transporting after task a, 0 means otherwise
$SoC_a^{C,tmax}$	State-of-Charge value at the end of task a if the electric vehicle is operated in charging state
$SoC_a^{C,tmin}$	State-of-Charge value at the beginning of task a if the electric vehicle is operated in charging state
$T_a^{C,D}$	Duration of charging state in task a if the electric vehicle is operated in charging state (second)
$T_a^{C,max}$	Time value at the end of task a if the electric vehicle is operated in charging state (second)
$T_a^{C,min}$	Time value at the beginning of task a if the electric vehicle is operated in charging state (second)
$U_{a,h}^{L,min}$	Binary variable for indicating the charging state in task a starts later than $T_h^{H,min}$; 1 means the charging state starts later than $T_h^{H,min}$, 0 means otherwise
$U_{a,h}^{E,min}$	Binary variable for indicating the charging state in task a starts earlier than $T_h^{H,max}$; 1 means the charging state starts earlier than $T_h^{H,max}$, 0 means otherwise
$U_{a,h}^{B,min}$	Binary variable for indicating the charging state in task a starts between $T_h^{H,min}$ and $T_h^{H,max}$; 1 means the charging state starts between $T_h^{H,min}$ and $T_h^{H,max}$, 0 means otherwise
$U_{a,h}^{L,max}$	Binary variable for indicating the charging state in task a ends later than $T_h^{H,min}$; 1 means the charging state ends later than $T_h^{H,min}$, 0 means otherwise
$U_{a,h}^{E,max}$	Binary variable for indicating the charging state in task a ends earlier than $T_h^{H,max}$; 1 means the charging state ends earlier than $T_h^{H,max}$, 0 means otherwise
$U_{a,h}^{B,max}$	Binary variable for indicating the charging state in task a ends between $T_h^{H,min}$ and $T_h^{H,max}$; 1 means the charging state ends between $T_h^{H,min}$ and $T_h^{H,max}$, 0 means otherwise
$SoC_a^{P,tmax}$	State-of-Charge value at the end of task a if the electric vehicle is operated in parking state
$SoC_a^{P,tmin}$	State-of-Charge value at the beginning of task a if the electric vehicle is operated in parking state
$T_a^{P,D}$	Duration of parking state in task a if the electric vehicle is operated in parking state (second)
$T_a^{P,max}$	Time value at the end of task a if the electric vehicle is operated in parking state (second)
$T_a^{P,min}$	Time value at the beginning of task a if the electric vehicle is operated in parking state (second)
$SoC_a^{T,tmax}$	State-of-Charge value at the end of task a if the electric vehicle is operated intransporting state
$SoC_a^{T,tmin}$	State-of-Charge value at the beginning of task a if the electric vehicle is operated in transporting state
$SoC_{a,n}^{N}$	State-of-Charge value when the electric vehicle arrives at node n in task a
$T_a^{T,D}$	Duration of parking state in task a if the electric vehicle is operated in transporting state (second)
$T_a^{T,max}$	Time value at the end of task a if the electric vehicle is operated in transporting state (second)
$T_a^{T,min}$	Time value at the beginning of task a if the electric vehicle is operated in transporting state (second)
$x_{a,l}^{ev}$	Binary variable for indicting edge selection in task a; 1 means edge l is taken in task a, 0 means otherwise
$T_{a,n}^{N}$	Time when the electric vehicle arrives at node n in task a (second)
$T_{a,c}^{DC}$	Time duration for delivering customer c in task a (second)
$V_{a,c}^{min}$	Binary variable for indicating the pickup time in task a is later than $T_c^{C,min}$; 1 means the pickup time is later than $T_c^{C,min}$, 0 means otherwise
$V_{a,c}^{max}$	Binary variable for indicating the pickup time in task a is earlier than $T_c^{C,max}$; 1 means the pickup time is earlier than $T_c^{C,max}$, 0 means otherwise
$V_{a,c}^{bet}$	Binary variable for indicating the pickup time of customer c is between $T_c^{C,min}$ and $T_c^{C,max}$; 1 means the pickup time is between $T_c^{C,min}$ and $T_c^{C,max}$ in task a, 0 means otherwise

Table 3
Nomenclature (cont').

$$\underset{\Xi}{\text{minimize}} \quad C_1 + C_2 + C_3 \tag{3}$$

$$\Xi = \Big\{C_1, C_2, C_3, S_a^{V,C}, S_a^{V,P}, S_a^{V,T}, D_a^{V,C}, D_a^{V,P}, D_a^{V,T}, SoC_a^{C,tmax}, SoC_a^{C,tmin}, T_a^{C,D} \\ T_a^{C,max}, T_a^{C,min}, U_{a,h}^{L,min}, T_h^{H,min}, U_{a,h}^{E,min}, T_h^{H,max}, U_{a,h}^{B,min}, U_{a,h}^{L,max}, U_{a,h}^{E,max}, U_{a,h}^{B,max}, \\ SoC_a^{P,tmax}, SoC_a^{P,tmin}, T_a^{P,D}, T_a^{P,max}, T_a^{P,min}, SoC_a^{T,tmax}, SoC_a^{T,tmin}, SoC_{a,n}^{N}, T_a^{T,D}, \\ T_a^{T,max}, T_a^{T,min}, x_{a,l}^{ev}, T_{a,n}^{N}\Big\} \tag{4}$$

$$\text{where } C_1 = \sum_{h,a} S_a^{V,C} U_{a,h}^{B,min} U_{a,h}^{B,max} Q^C P_h \left(T_a^{C,max} - T_a^{C,min}\right) \tag{5}$$

$$C_2 = \sum_{h,a} S_a^{V,C} U_{a,h}^{B,min} U_{a,h+1}^{B,max} \left[Q^C P_h \left(T_h^{H,max} - T_a^{C,min}\right) + Q^C P_{h+1} \left(T_a^{C,max} - T_{h+1}^{H,min}\right)\right] \tag{6}$$

$$C_3 = \omega \sum_{a,c} S_a^{V,T} T_{a,c}^{DC} \tag{7}$$

$Q_{a,c}$	Binary variable for indicating the dropoff time is greater than pickup time for customer c; 1 means for customer c in task a, its dropoff time is later than pickup time, 0 means otherwise
$V_{a,n}^{PN}$	Binary variable for indicating the electric vehicle passes the node n in task a; 1 means the electric vehicle passes the node n in task a

time value is within the time period h, as enforced by (15)-(17).

3.2.2. The relevant constraints of parking state (state 2)

The relevant constraints of parking state are elaborated as follows:

$$-M\left(1 - S_a^{V,P}\right) \le SoC_a^{P,tmax} - SoC_a^{P,tmin} \le M\left(1 - S_a^{V,P}\right), \quad \forall a \in \Phi^{EA} \tag{18}$$

$$-M\left(1 - S_a^{V,P}\right) \le T_a^{P,max} - \left(T_a^{P,min} + T_a^{P,D}\right) \le M\left(1 - S_a^{V,P}\right), \ \forall a \in \Phi^{EA} \tag{19}$$

$$SoC_a^{P,tmax} S_a^{V,P} \le SoC^{max} S_a^{V,P}, \quad \forall a \in \Phi^{EA} \tag{20}$$

$$SoC_a^{P,tmin} S_a^{V,P} \ge SoC^{min} S_a^{V,P}, \quad \forall a \in \Phi^{EA} \tag{21}$$

Constraint (18) shows that SoC value remains constant during parking state. Constraint (19) imposes the time evolution constraint of parking state. Constraints (20) and (21) enforce the SoC value bounds for parking state if the parking state is selected ($S_a^{V,P} = 1$).

3.2.3. The relevant constraints of transporting state (state 3)

The relevant constraints of transporting state are elaborated as follows.

$$-M\left(1-S_a^{V,T}\right)\le T_a^{T,max}-\left(T_a^{T,min}+T_a^{T,D}\right)\le M\left(1-S_a^{V,T}\right),\ \forall a\in\Phi^{EA} \tag{22}$$

Constraint (22) presents the time evolution constraint of transporting state.

$$SoC_a^{T,tmin}S_a^{V,T}\le SoC^{max}S_a^{V,T},\quad \forall a\in\Phi^{EA} \tag{23}$$

$$SoC_a^{T,tmax}S_a^{V,T}\ge SoC^{min}S_a^{V,T},\quad \forall a\in\Phi^{EA} \tag{24}$$

Constraints (23) and (24) enforce upper and lower bounds of *SoC*value in transporting state.

$$\sum_{l\in\Omega^{HU}\cup\Omega^{HD}} x_{a,l}^{ev}S_a^{V,T}\ge 1,\quad \forall a\in\Phi^{EA} \tag{25}$$

The home node (*HN*) is the starting and ending node of every itinerary of transporting state, therefore at least one path must be leading away and leading to it, as indicated in (25). In other words, at least one edge connected to the home node ($\Omega^{HU}\cup\Omega^{HD}$) must be taken.

$$\left(\sum_{a,l\in\Omega_n^{U,L}} x_{a,l}^{ev}-\sum_{a,l\in\Omega_n^{D,L}} x_{a,l}^{ev}\right)S_a^{V,T}=0,\quad \forall n\in N,a\in\Phi^{EA} \tag{26}$$

Constraint (26) indicates that if the EV enters (exits) a non-home node, it must lead away from (to) this node afterward (beforehand). In other words, for a non-home node *n*, the number of taken upstream edges ($\sum_{a,l\in\Omega_n^{U,L}} x_{a,l}^{ev}$) must be equal to the number of taken downstream edges ($\sum_{a,l\in\Omega_n^{D,L}} x_{a,l}^{ev}$).

$$-M\left(1-V_{a,n}^{PN}\right)S_a^{V,T}\le\left(\sum_{a,l\in\Omega_n^{U,L}} x_{a,l}^{ev}+\sum_{a,l\in\Omega_n^{D,L}} x_{a,l}^{ev}-1\right)S_a^{V,T}\le MV_{a,n}^{PN}S_a^{V,T},\quad \forall n\in N,a\in\Phi^{EA} \tag{27}$$

Constraint (27) determines the value of $V_{a,n}^{PN}$, which indicates whether node *n* is passed or not. If node *n* is passed, at least one of its upstream ($\sum_{a,l\in\Omega_n^{U,L}}$) and downstream edges ($\sum_{a,l\in\Omega_n^{D,L}}$) must be taken.

$$-MS_a^{V,T}\left(1-x_{a,l}^{ev}\right)\le S_a^{V,T}\left(\sum_{a,l\in\Omega_l^{D,N}} T_{a,n}^{N}V_{a,n}^{PN}+\tau_l-\sum_{a,l\in\Omega_l^{U,N}} T_{a,n}^{N}V_{a,n}^{PN}\right)\le MS_a^{V,T}\left(1-x_{a,l}^{ev}\right),\quad \forall l\in L,a\in\Phi^{EA} \tag{28}$$

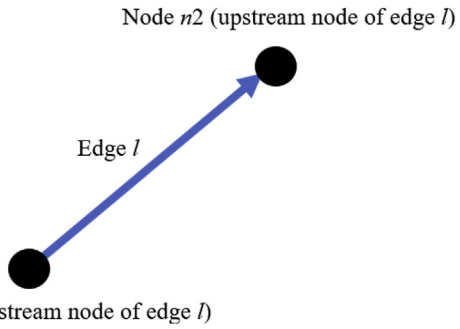

Fig. 3. Time and SoC evolution illustration.

$$-MS_a^{V,T}\left(1-V_{a,c}^{min}\right)\le S_a^{V,T}\left(\sum_{\Omega_c^{P,N}} T_{a,n}^{N}V_{a,n}^{PN}-T_c^{C,min}\right)\le MS_a^{V,T}V_{a,c}^{min},\quad \forall a\in\Phi^{EA},c\in C \tag{30}$$

$$-MS_a^{V,T}\left(1-V_{a,c}^{max}\right)\le S_a^{V,T}\left(-\sum_{\Omega_c^{P,N}} T_{a,n}^{N}V_{a,n}^{PN}+T_c^{C,max}\right)\le MS_a^{V,T}V_{a,c}^{max},\quad \forall a\in\Phi^{EA},c\in C \tag{31}$$

$$V_{a,c}^{bet}=V_{a,c}^{max}V_{a,c}^{min},\quad \forall a\in\Phi^{EA},c\in C \tag{32}$$

$$-MS_a^{V,T}\left(1-x_{a,l}^{ev}\right)\le S_a^{V,T}\left(\sum_{a,l\in\Omega_l^{D,N}} SoC_{a,n}^{N}-E_l\Big/E^{max}-\sum_{a,l\in\Omega_l^{U,N}} SoC_{a,n}^{N}\right)\le MS_a^{V,T}\left(1-x_{a,l}^{ev}\right)\ \forall l\in L,a\in\Phi^{EA} \tag{29}$$

Constraint (28) presents the evolution of arrival time at each node. As seen, the arrival time of a node *n* ($\sum_{a,l\in\Omega_l^{U,N}} T_{a,n}^{N}V_{a,n}^{PN}$) is determined by the arrival time of the previous node ($\sum_{a,l\in\Omega_l^{D,N}} T_{a,n}^{N}V_{a,n}^{PN}$) and time consumption of the connecting edge (τ_l). Fig. 3 illustrates the evolving process working in the same manner for both time and SoC. The node *n*2is defined as the upstream of the edge *l*, while the previous node *n*1is the downstream node of the edge *l*. Obviously, the arrival time of *n*2should be the arrival time of *n*1plus the time consumption on *l*. Multiplying $V_{a,n}^{PN}$ to arrival times enforces the arrival times of unpassed nodes to zero. Similarly, constraint (29) presents the evolution of *SoC*value at each node, as the *SoC*value at node *n*2is determined by the *SoC*value at the

previous node ($n1$) and SoCconsumption on edge l.

Constraints (30)–(32) determine pickup indicator of customers ($V_{a,c}^{bet}$). Specifically, the arrival time at pickup node should be within the time window of picking up customers. The binary variable $V_{a,c}^{min}$determines whether the arrival time at pickup node is later than the start point of pickup time window ($T_c^{C,min}$), as imposed by (30). Similarly, the binary variable $V_{a,c}^{max}$denotes whether the arrival time at pickup node is earlier than the end point of pickup time window ($T_c^{C,max}$), as imposed by (31). When the pickup time is earlier/later than the starting/ending time of the required time window, the customer is picked up successfully, as indicated in (32).

$$-MS_a^{V,T}(1-Q_{a,c}) \le S_a^{V,T}\left(\sum_{\Omega_c^{D,N}} T_{a,n}^N V_{a,n}^{PN} - \sum_{\Omega_c^{P,N}} T_{a,n}^N V_{a,n}^{PN}\right) \le MS_a^{V,T}Q_{a,c}, \quad \forall a\in\Phi^{EA}, c\in C \tag{33}$$

Constraint (33) determines the value of $Q_{a,c}$ that indicates whether the arrival time at dropoff node ($\sum_{\Omega_c^{D,N}} T_{a,n}^N V_{a,n}^{PN}$) is later than the arrival time of pickup node ($\sum_{\Omega_c^{P,N}} T_{a,n}^N V_{a,n}^{PN}$). Obviously, only if $Q_{a,c}=1$, the customer is successfully delivered. Multiplying $V_{a,n}^{PN}$is to enforce arrival time of unpassed nodes to zero. The *if – else*statement III is applied here.

3.2.4. The supplementary constraints

The supplementary constraints are the sets of constraints that define interconnections between states and overall requirements, which are elaborated as follows.

$$S_{a+1}^{V,C} = \left(S_a^{V,P} + S_a^{V,T}\right)D_a^{V,C}, \quad \forall a\in\Phi^{EA}, c\in C \tag{34}$$

$$S_{a+1}^{V,P} = \left(S_a^{V,C} + S_a^{V,T}\right)D_a^{V,P}, \quad \forall a\in\Phi^{EA}, c\in C \tag{35}$$

$$S_{a+1}^{V,T} = \left(S_a^{V,C} + S_a^{V,P}\right)D_a^{V,T}, \quad \forall a\in\Phi^{EA}, c\in C \tag{36}$$

Constraints (34) - (36) impose a series of constraints for state transition, which correspond to the diagram depicted in Fig. 1(a).

$$-M\left(1-S_a^{V,C}\right) \le SoC_{a+1}^{C,tmin} - \left(S_a^{V,P}D_a^{V,C}SoC_a^{P,tmax} + S_a^{V,T}D_a^{V,C}SoC_a^{T,tmax}\right) \le M\left(1-S_a^{V,C}\right), \ \forall a\in\Phi^{EA} \tag{37}$$

$$-M\left(1-S_a^{V,P}\right) \le SoC_{a+1}^{P,tmin} - \left(S_a^{V,C}D_a^{V,P}SoC_a^{C,tmax} + S_a^{V,T}D_a^{V,P}SoC_a^{T,tmax}\right) \le M\left(1-S_a^{V,P}\right), \ \forall a\in\Phi^{EA} \tag{38}$$

$$-M\left(1-S_a^{V,T}\right) \le SoC_{a+1}^{T,tmin} - \left(S_a^{V,C}D_a^{V,T}SoC_a^{C,tmax} + S_a^{V,P}D_a^{V,T}SoC_a^{P,tmax}\right) \le M\left(1-S_a^{V,T}\right), \ \forall a\in\Phi^{EA} \tag{39}$$

$$-M\left(1-S_a^{V,C}\right) \le T_{a+1}^{C,tmin} - \left(S_a^{V,P}D_a^{V,C}T_a^{P,tmax} + S_a^{V,T}D_a^{V,C}T_a^{T,tmax}\right) \le M\left(1-S_a^{V,C}\right), \ \forall a\in\Phi^{EA} \tag{40}$$

$$-M\left(1-S_a^{V,P}\right) \le T_{a+1}^{P,tmin} - \left(S_a^{V,C}D_a^{V,P}T_a^{C,tmax} + S_a^{V,T}D_a^{V,P}T_a^{T,tmax}\right) \le M\left(1-S_a^{V,P}\right), \quad \forall a\in\Phi^{EA} \tag{41}$$

$$-M\left(1-S_a^{V,T}\right) \le T_{a+1}^{T,tmin} - \left(S_a^{V,C}D_a^{V,T}T_a^{C,tmax} + S_a^{V,P}D_a^{V,T}T_a^{P,tmax}\right) \le M\left(1-S_a^{V,T}\right), \quad \forall a\in\Phi^{EA} \tag{42}$$

Furthermore, state transitions define the inter-state changes of SoCvalues and time evolution between sequential states, as formulated by constraints (37)–(42). Specifically, the initial values of $SoC$and time of the current state is determined by the final $SoC$and time values of the previous state, as imposed by constraints (37)–(39) and (40)–(42), respectively.

$$S_a^{V,C} + S_a^{V,P} + S_a^{V,T} = 1, \quad \forall a\in\Phi^{EA} \tag{43}$$

$$D_a^{V,C} + D_a^{V,P} + D_a^{V,T} = 1, \quad \forall a\in\Phi^{EA} \tag{44}$$

Constraints (43) shows that for each task, only one state will be selected. Moreover, (44) denotes that only one action will be taken after each ongoing task.

$$SoC_{a1}^{C,tmin}S_{a1}^{V,C} + SoC_{a1}^{P,tmin}S_{a1}^{V,P} + SoC_{a1}^{T,tmin}S_{a1}^{V,T} = SoC^{ini} \tag{45}$$

$$T_{a1}^{C,min}S_{a1}^{V,C} + T_{a1}^{P,min}S_{a1}^{V,P} + T_{a1}^{T,min}S_{a1}^{V,T} = 0 \tag{46}$$

Constraints (45) and (46) define the initial time and SoCvalues in the first task.

$$SoC_{a1}^{C,tmax}S_{a1}^{V,C} + SoC_{a1}^{P,tmax}S_{a1}^{V,P} + SoC_{a1}^{T,tmax}S_{a1}^{V,T} = SoC^{ini} \tag{47}$$

$$T_{a1}^{C,max}S_{a1}^{V,C} + T_{a1}^{P,max}S_{a1}^{V,P} + T_{a1}^{T,max}S_{a1}^{V,T} \le T^{max} \tag{48}$$

Constraints (47) and (48) define the final time and SoCvalues in the final task of the entire time horizon. Note that constraints (45) and (47) ensure that battery SoCvalue remains the same after the entire time horizon.

$$\sum_a Q_{a,c}V_{a,c}^{bet} = 1, \forall c\in C \tag{49}$$

Constraint (49) indicates that each customer must be served. Specifically, with $V_{a,c}^{bet}=1$, the customer can be picked up at the right place and right time. Further, $Q_{a,c}=1$means that the customer is delivered successfully. These two conditions together ensure the proper services of all the customers.

$$WT \le \sum_a T_a^{C,D}S_a^{V,C} + T_a^{P,D}S_a^{V,P} \tag{50}$$

Finally, constraint (50) ensures the sufficient working time duration. Note that in this model, there exist products of binary variables, as well as products of a binary variable and a positive continuous variable. To eliminate the non-linearities, these products of variables need to be linearized. Reference [22] gives detailed

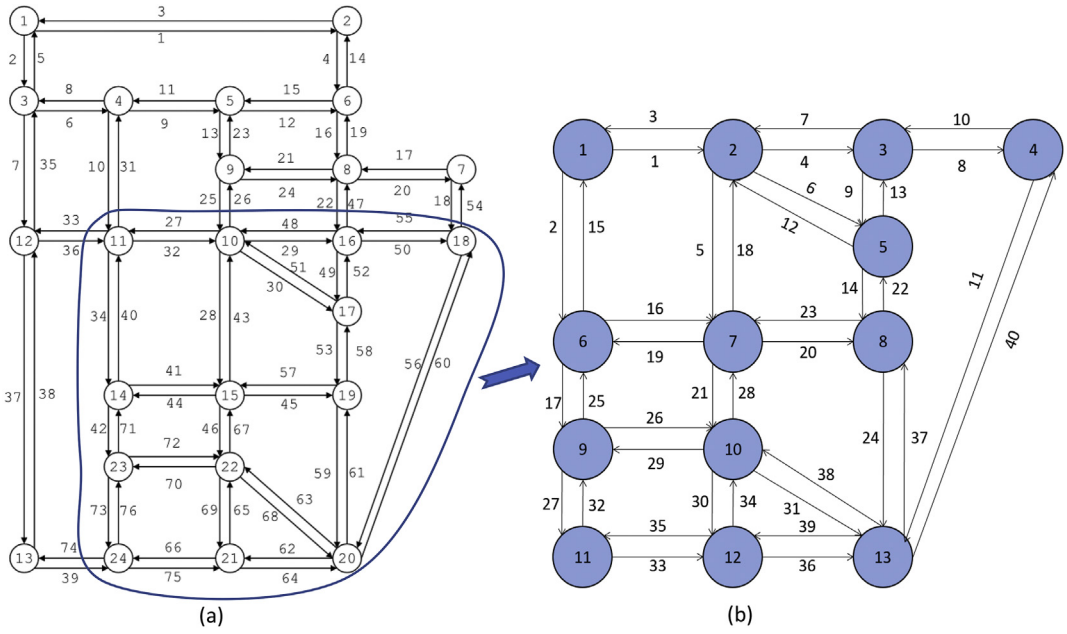

Fig. 4. Transportation nodes topology networks, (a) original Sioux Falls network, (b) reduced Sioux Falls network.

linearization method for these bilinear terms. After linearization, the model can be reformulated into a mixed-integer linear programming (MILP) model, in which global optimal solution can be guaranteed by commercial branch-and-cut algorithm based solvers, such as CPLEX, Gurobi, among others. Specifically, branch-and-cut algorithm implements "divide and conquer" strategy to derive the optimal solutions of MILP problems by relaxing integer variables and cutting feasible regions iteratively. Detailed introduction about branch-and-cut algorithm and corresponding commercial solvers can be found in Ref. [23–25].

4. Case study

This section demonstrates the proposed model by presenting numerical results based on a realistic transportation network of the city Sioux Falls, South Dakota, whose data is readily available [26]. Fig. 4 (a) depicts the corresponding topology with 24 nodes and 76 edges. Since the research aim of this paper is to address EV scheduling in a small region, we reduce the network into a reduced version with 13 nodes and 40 edges, as presented in Fig. 4 (b).

Furthermore, we assume three customers to serve, and the entire time horizon is 8 h. It is also assumed that charging price (CP) changes every 2 h. Additionally, the home of EV initial position is located at node 1 in Fig. 4 (b), and the initial weighting term ω is set to be 0.02. The sensitivity analysis of ω on model performance will be tested later on. Further, the capacity of EV battery is assumed to be 100 kWh, which corresponds to normal capacity of the battery pack installed in Tesla Model X [27], and the charging rate is fixed as 12 kW/h. Note that the proposed model has a good generalization capability and can be easily applied for other scenarios with different parameters. All the optimization models are implemented in General Algebraic Modeling System (GAMS) environment, using a laptop with an Intel Core i7 CPU and 16 GB RAM. CPLEX is selected as the underlying solver for the proposed MILP optimization problem. Parameters of the road transportation network are summarized in Ref. [26].

The time (τ_l) and energy (E_l) consumption of each road l are computed by equations (51) and (52) [6].

$$\tau_l = \tau_l^F(1 + \alpha(V_l/C_l)^\beta) \tag{51}$$

In (51), τ_l^F stands for free flow time, V_l for traffic flow and C_l for road capacity. α and β are experimental coefficients from realistic observations, which are assumed to be 0.15 and 4 respectively in this paper [6].

$$E_l = Fd_l \tag{52}$$

In (52), F is the total longitudinal force or tractive force of EVs that is in positive correlation with EVs speed, and d_l denotes the distance of road l. The resultant time and energy consumption of roads are summarized in Refs. [28].

4.1. The effect of charging price scenarios

The effects of charging price on model outcomes are evaluated as follows. In this case, we will examine the model performance under three different scenarios of charging prices, which are tabulated in Table 4. Additionally, in this case, three customers need to be transported and pickup/dropoff nodes of them are N6/N13, N12/N4, and N2/N6, respectively. First of all, we can observe 8 tasks throughout entire time horizon, with 3 tasks are assigned to transporting state for delivering three customers, 2 tasks are assigned to charging state for replenishing EV battery energy consumption, and 3 tasks are assigned to parking state as the intermediate tasks. Additionally, it can be seen that charging state is deliberately assigned to the time periods with relatively lower charging price. For instance, for scenario 1, the charging state is assigned in the earlier tasks and time periods, i.e. tasks 1 (0:00–70:20) and 3 (105:00–172:46), since charging price increases along the time for this particular scenario, as shown in Fig. 5(a). However, when charging price decreases along the time (scenario 2), EV battery will be charged in the later tasks and time periods, i.e. Task 5 and 7 at time periods of 278:35–384:57 and 406:21–438:05, as shown in Fig. 5(b). Therefore, we can conclude that the proposed model enables price-responsive charging schemes that schedule charging activities at the time slots with

Table 4
Scenarios of charging prices.

	CP (0:00–2:00)	CP (2:00–4:00)	CP (4:00–6:00)	CP (6:00–8:00)
Scenario 1	38 ($/MWh)	48 ($/MWh)	53 ($/MWh)	70 ($/MWh)
Scenario 2	70 ($/MWh)	53 ($/MWh)	48 ($/MWh)	38 ($/MWh)
Scenario 3	70 ($/MWh)	38 ($/MWh)	48 ($/MWh)	53 ($/MWh)
Scenario 4	38 ($/MWh)	70 ($/MWh)	53 ($/MWh)	48 ($/MWh)

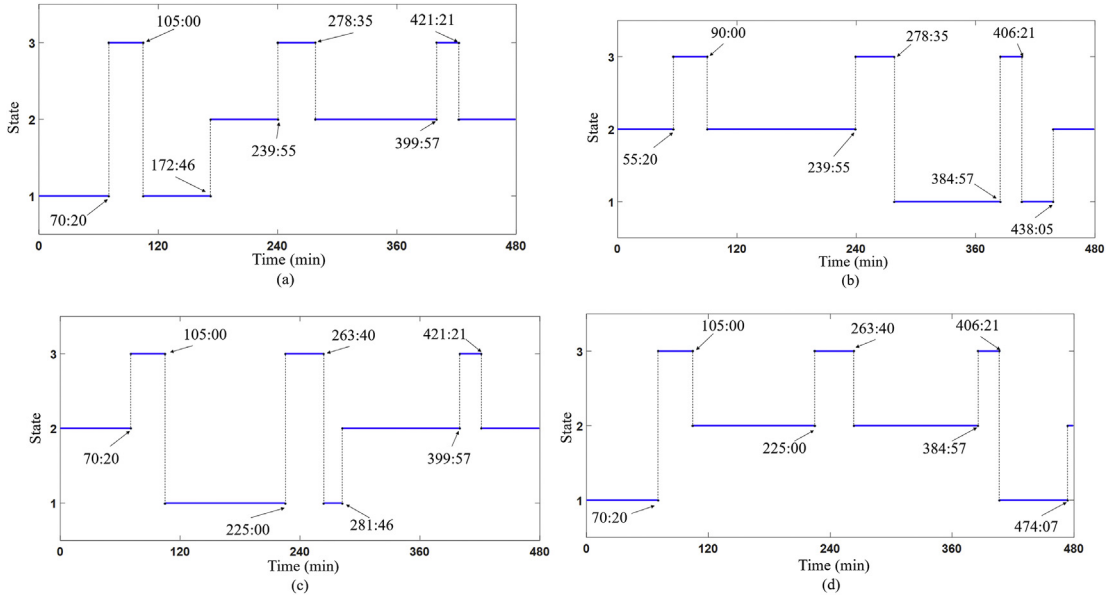

Fig. 5. State evolution in process of time with various charging price scenarios indicated in Table 4, (a) charging price scenario 1, (b) charging price scenario 2, (c) charging price scenario 3, (d) charging price scenario 4.

lower charging prices. To visualize the optimal routing result, Fig. 6 depicts route selections for transporting states. These results demonstrates the geographically successful deliveries of customers, as pickup nodes are passed before dropoff nodes. The timely pickups of customers will be demonstrated in the following subsection .

4.2. The effects of customers behaviors

In the section, we examine the effects of customers behaviors, including pickup/dropoff locations and pickup times of customers, on model outcomes. Firstly, routes with the same pickup time window but different scenarios of pickup/dropoff locations will be obtained. Assuming three customers are expected to be picked up at 60:00–75:00, 240:00–255:00, and 390:00–405:00. Table 5 presents pickup/dropoff locations of three customers for different scenarios. Accordingly, all the EV itineraries are determined as tabulated in Table 6, in which pickup and dropoff nodes are highlighted by red and green color, respectively.

As seen, each itinerary is determined according to customers demands beforehand, including pickup/dropoff locations and pickup time windows. Specifically, the pickup nodes are passed before dropoff nodes for all scenarios. Besides, the pickup times of customers are scheduled within the time windows determined by customers' demands.

Furthermore, state assignments in sequential tasks, along with the corresponding time values, and different pickup time windows scenarios are presented in Fig. 7. In this demonstration, we assume that pickup/dropoff nodes of customer 1, 2, 3 are N7/N4, N12/N6, and N2/N13, respectively. Requested pickup time for two scenarios are tabulated in Table 7. Different state assignments can be witnessed for two pickup time scenarios since the overall schedule needs to be adjusted to leave the proper time windows for picking up customers, which shows the effects of customers behavior on the EV scheduling. It should be noted that the starting time of transporting states do not imply the pickup time, since the process of driving from the starting node to the pickup node consumes certain time. In the following subsection, we will examine the effects of decision maker's preference on the model outcome.

4.3. The effects of weighting term

The weighting term ω in the objective function (1) determines the decision maker's preference on minimizing total customers delivery time. To demonstrate effects of weighting term on model outcome, we intentionally reduce the time consumption of 8 edges in the transportation network while increase the energy consumption of them, as summarized in Table 8. These modifications are reasonable in practice, since energy consumption usually increases with vehicle velocity while time consumption is inversely proportional to vehicle velocity [6].

Route selections of customers 1 and 3 are depicted in Figs. 8 and 9, with different values of ω. As seen in these figures, when the value of ω is higher, the vehicle will choose edges with less time consumption to reduce delivery times of customers at the expense of higher energy consumption. For instance, for customer 1, the EV would select route $16 \rightarrow 21 \rightarrow 31$, rather than route $17 \rightarrow 27 \rightarrow 33 \rightarrow 36$with $\omega = 0.5$for the sake of customers delivery times reduction, despite of its higher energy consumption. These route adjustments are due to the decision maker's higher

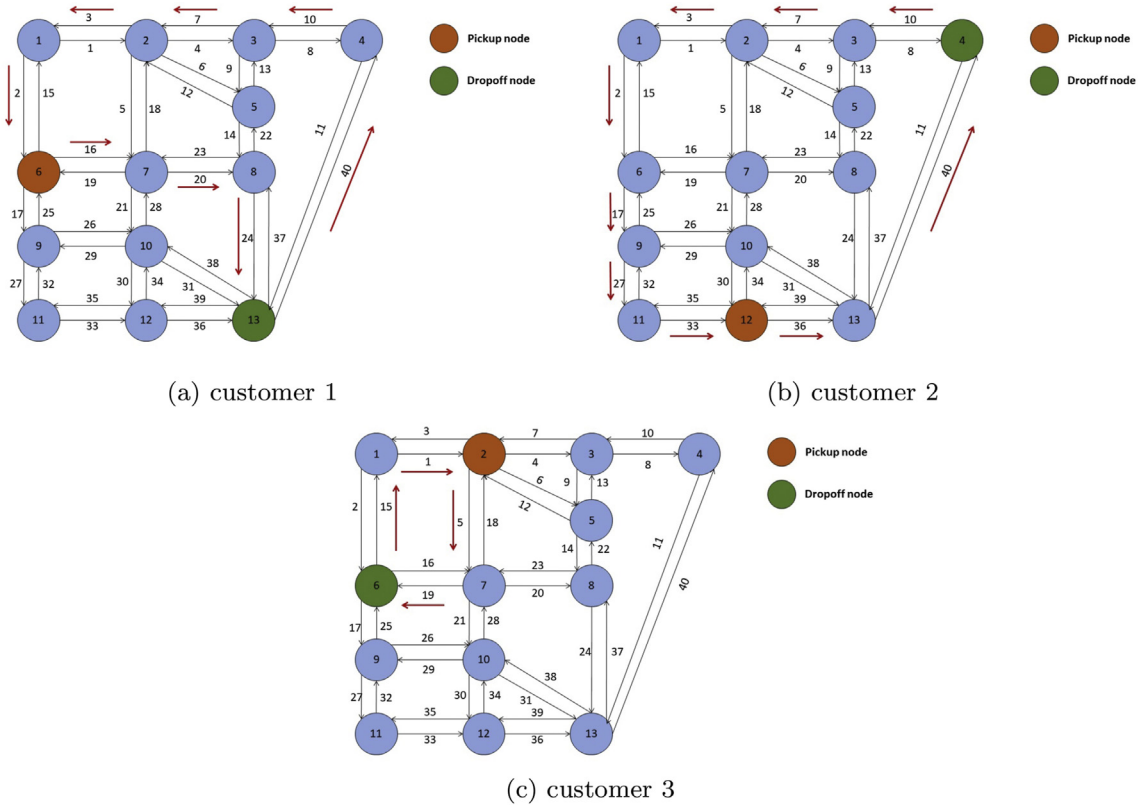

Fig. 6. Routing of transporting state for delivering customers with pickup/dropoff nodes of N6/N13, N12/N4, and N2/N6, (a) customer 1, (b) customer 2, (c) customer 3.

Table 5
Pickup/dropoff locations of customers for different scenarios.

		Pickup/Dropoff nodes		Pickup/Dropoff nodes		Pickup/Dropoff nodes
Scenario 1	Customer 1	N13/N3	Customer 2	N11/N8	Customer 3	N4/N6
Scenario 2	Customer 1	N7/N4	Customer 2	N12/N6	Customer 3	N5/N9
Scenario 3	Customer 1	N2/N11	Customer 2	N3/N13	Customer 3	N12/N4

Table 6
Customer itineraries for different scenarios.

		Itinerary
Scenario 1	Customer 1	N1→ N6→ N7→ N8→ N13 (60:00) → N4→ N3→ N2→ N1
Scenario 1	Customer 2	N1→ N6→ N9→ N11 (255:00) → N12→ N10 N N7→ N8→ N5→ N3→ N2→ N1
Scenario 1	Customer 3	N1→ N2→ N3→ N4 (390:00) →N13→ N8 N N15→ N6→ N1
Scenario 2	Customer 1	N1→ N6→ N7 (75:00) →N8→ N13→ N4→ N3→ N2→ N1
Scenario 2	Customer 2	N1→ N2→ N7→ N10→ N12 (242:28) →N11→ N9→ N6→ N1
Scenario 2	Customer 3	N1→ N2→ N3→ N5 (405:00) →N8→ N7→ N10→ N9→ N6→ N1
Scenario 3	Customer 1	N1→ N2 (73:15) →N7→ N10→ N12→ N11→ N9 →N6→ N1
Scenario 3	Customer 2	N1→ N2→ N3 (249:43) →N4→ N13→ N8→ N7→ N6→ N1

preference over reducing customers' delivery times, thus the routes with less time consumption, despite higher energy consumption, are selected.

4.4. Cost benefits

This subsection demonstrates the merits of the proposed approach for EV car-sharing scheduling via conducting a series of comparison studies. To begin with, the total costs of three approaches are summarized for comparison in Table 9 as follows:

Approach A: The car-sharing EV scheduling is determined by solving the proposed model using CPLEX solver.
Approach B: The EV enters charging states after delivering a customer, till its SoC value reaches the initial SoC value.
Approach C: The car-sharing EV scheduling is determined by solving the proposed model using a widely adopted heuristic solution technique, i.e. Particle Swarm Optimization (PSO), which is inspired by the swarming strategies of various organisms in nature to iteratively locate the improved solution candidates [29].

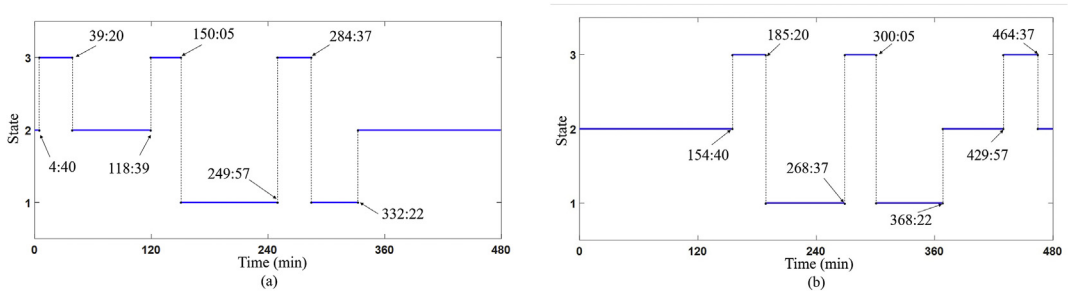

Fig. 7. State evolution in process of time with various customers pickup time scenarios indicated in Table 7, (a) customer pickup time scenario 1, (b) customer pickup time scenario 2.

Table 7
Pickup time for different customers and scenarios.

		Pickup time		Pickup time		Pickup time
Scenario 1	Customer1	15:00–30:00	Customer 2	135:00–150:00	Customer 3	255:00–270:00
Scenario 2	Customer1	165:00–180:00	Customer 2	285:00–300:00	Customer 3	420:00–435:00

Table 8
Edges parameters modification.

Energy consumption (kWh)			Time consumption (min)		
Edge	Original system	Revised system	Edge	Original system	Revised system
L6	2.54	4.65	L6	9.21	5.07
L11	1.27	4.38	L11	4	2.27
L12	2.54	4.65	L12	9.21	5.07
L16	1.59	4.1	L16	5.68	2.82
L19	1.59	4.1	L19	5.68	2.82
L31	1.65	4.15	L31	5.71	2.89
L38	1.65	4.15	L38	5.71	2.89
L40	1.27	4.02	L40	4	2.27

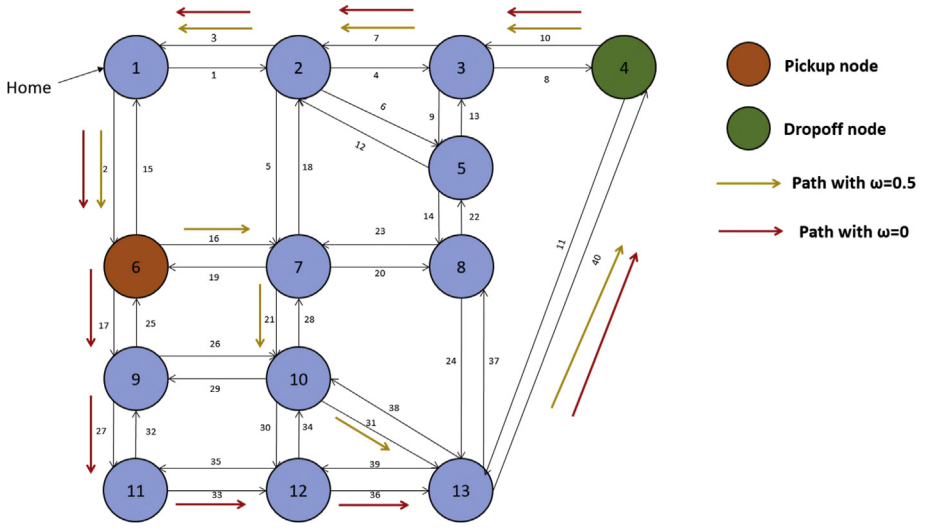

Fig. 8. Optimal route selection with different values of ω for customer 1, with higher value of ω implies higher preference for customer delivery time reduction.

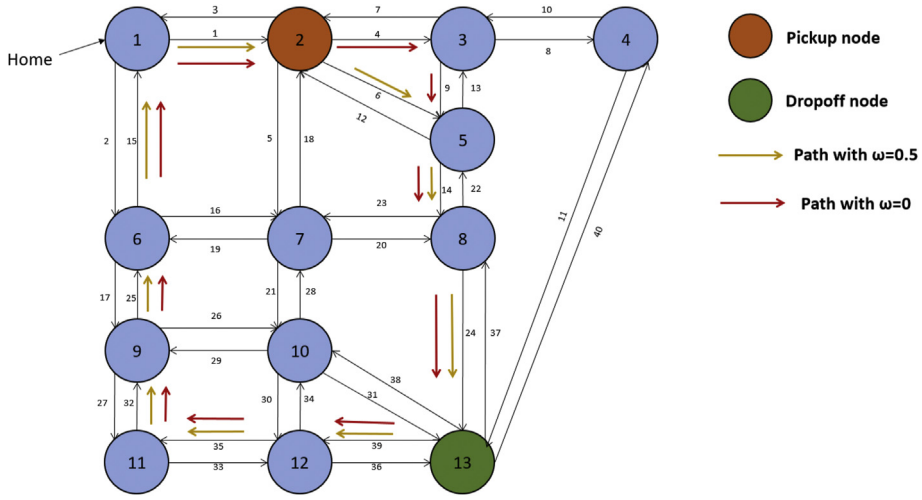

Fig. 9. Optimal route selection with different values of ω for customer 3, with higher value of ω implies higher preference for customer delivery time reduction.

Table 9
Total cost comparison with different charging price scenarios among various approaches.

	Approach A	Approach B	Approach C
Scenario 1	1.872	2.295	2.004
Scenario 2	1.929	2.187	2.341
Scenario 3	1.898	1.898	2.659
Scenario 4	1.902	2.199	3.769

Table 10
Charging cost comparison with different charging price scenarios between approaches A and B.

	Approach A	Approach B
Scenario 1	$0.897	$1.32
Scenario 2	$0.954	$1.212
Scenario 3	$0.923	$0.923
Scenario 4	$0.927	$1.224

Table 9 summarizes cost comparisons between three approaches for case studies with a variety of charging cost scenarios indicated in Table 4. The comparison between approaches A and B indicates that up to 18.5% cost saving can be accomplished by adopting the proposed model, which validates cost benefit of the proposed model. This is mainly because of the strategic allocation of time slots for EV charging that leads to lower charging cost, as witnessed in Table 10. Additionally, Fig. 10 depicts the state evolution in the process of time with approaches A and B for the charging price scenario 1, as an example, along with charging price trend. As seen, if the proposed approach is applied, the EV charging activity (state 1) can be scheduled to the periods with lower charging price deliberately, without violating other constraints.

Furthermore, the cost comparison between approaches A and C, as shown in Table 9, validates the advantage and necessity of recasting the proposed model into a MILP problem and using a branch-and-cut algorithm based solver (e.g. CPLEX) to obtain the global optimal solution. It can be seen that total cost saving by adopting approach A, instead of approach C, could reach up to 49.5%.

5. Conclusion and future works

This paper proposes an optimization model for optimal routing and charging scheduling of EV car-sharing service, considering multi-temporal and multi-task operation. In particular, the proposed model is designed for EV owners, who seek to share the vehicle in a cost-effective manner while ensure sufficient working hours on a telecommuting job at home. The proposed model formulates the decision-making process for various EV states (i.e. charging, parking, transporting), as well as additional constraints representing state transitions, working hour requirement and energy neutral position of EV battery. The numerical studies

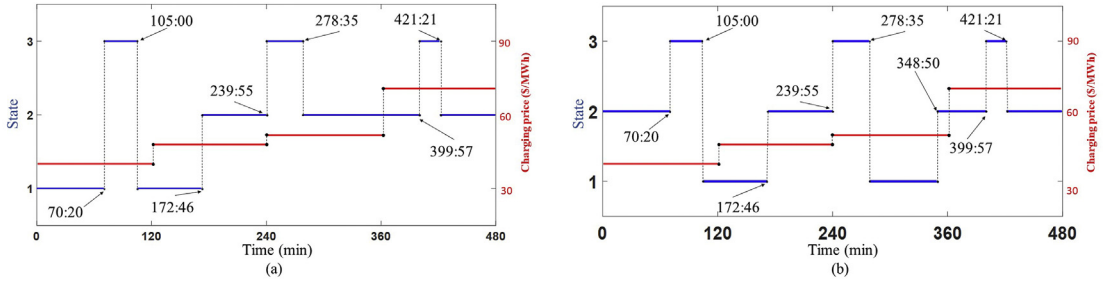

Fig. 10. State evolution in process of time with charging cost scenario 1 indicated in Table 4 with, (a) Approach A, (b) Approach B.

demonstrate the effectiveness of the proposed model and economic benefits of the proposed business mechanism in optimizing routing selection and charging strategy, as up to 18.5% cost saving can be accomplished compared to a baseline method. In the future, decomposition methods and learning algorithms will be incorporated to improve the efficiency of solution techniques, which would extend the proposed model to more flexible business paradigms and scenarios. Moreover, the compatibility and complementarity of proposed business model with other transport services, such as cargo delivery and hourly-paid car rental, etc., will be further discussed for enabling a highly electrified smart transportation system.

References

[1] Keller V, Lyseng B, Wade C, Scholtysik S, Fowler M, Donald J, Palmer-Wilson K, Robertson B, Wild P, Rowe A. Electricity system and emission impact of direct and indirect electrification of heavy-duty transportation. Energy 2019;172:740–51.

[2] Babar M, Arif F. Real-time data processing scheme using big data analytics in internet of things based smart transportation environment. Journal of Ambient Intelligence and Humanized Computing 2019;10(10):4167–77.

[3] Jadun P. The electrification futures study: transportation electrification, Tech. rep.. Golden, CO (United States): National Renewable Energy Lab.(NREL); 2019.

[4] Mamalis T, Bose S, Varshney LR. Ridesharing systems with electric vehicles. 2019 American control conference (ACC). IEEE; 2019. p. 3329–34.

[5] Montoya A, Guéret C, Mendoza JE, Villegas JG. The electric vehicle routing problem with nonlinear charging function. Transp Res Part B Methodol 2017;103:87–110.

[6] Chen T, Zhang B, Pourbabak H, Kavousi-Fard A, Su W. Optimal routing and charging of an electric vehicle fleet for high-efficiency dynamic transit systems. IEEE Transactions on Smart Grid 2016;9(4):3563–72.

[7] Lillebo M, Zaferanlouei S, Zecchino A, Farahmand H. Impact of large-scale ev integration and fast chargers in a Norwegian lv grid. J Eng 2019;(18):5104–8. 2019.

[8] Juul N, Meibom P. Optimal configuration of an integrated power and transport system. Energy 2011;36(5):3523–30.

[9] Liu Z, Wen F, Ledwich G. Optimal planning of electric-vehicle charging stations in distribution systems. IEEE Trans Power Deliv 2012;28(1):102–10.

[10] Tehrani NH, Wang P. Probabilistic estimation of plug-in electric vehicles charging load profile. Elec Power Syst Res 2015;124:133–43.

[11] Tang D, Wang P. Nodal impact assessment and alleviation of moving electric vehicle loads: from traffic flow to power flow. IEEE Trans Power Syst 2016;31(6):4231–42.

[12] Kong W, Luo Y, Feng G, Li K, Peng H. Optimal location planning method of fast charging station for electric vehicles considering operators, drivers, vehicles, traffic flow and power grid. Energy 2019;186:115826.

[13] Iacobucci R, McLellan B, Tezuka T. Modeling shared autonomous electric vehicles: potential for transport and power grid integration. Energy 2018;158:148–63.

[14] Keskin M, Çatay B. Partial recharge strategies for the electric vehicle routing problem with time windows. Transport Res C Emerg Technol 2016;65:111–27.

[15] Pelletier S, Jabali O, Laporte G. The electric vehicle routing problem with energy consumption uncertainty. Transp Res Part B Methodol 2019;126:225–55.

[16] Froger A, Mendoza JE, Jabali O, Laporte G. Improved formulations and algorithmic components for the electric vehicle routing problem with nonlinear charging functions. Comput Oper Res 2019;104:256–94.

[17] Yang H, Deng Y, Qiu J, Li M, Lai M, Dong ZY. Electric vehicle route selection and charging navigation strategy based on crowd sensing. IEEE Transactions on Industrial Informatics 2017;13(5):2214–26.

[18] Basso R, Kulcsár B, Egardt B, Lindroth P, Sanchez-Diaz I. Energy consumption estimation integrated into the electric vehicle routing problem. Transport Res Transport Environ 2019;69:141–67.

[19] Shi J, Gao Y, Wang W, Yu N, Ioannou PA. Operating electric vehicle fleet for ride-hailing services with reinforcement learning. IEEE Trans Intell Transport Syst 2019. https://doi.org/10.1109/TITS.2019.2947408 [Early Access].

[20] With $36 million in financing, scoop wants to make carpooling mainstream. https://www.forbes.com/sites/miguelhelft/2017/11/08/with-36-million-in-financing-scoop-wants-to-make-carpooling-mainstream/#ac2761f5e027; 2019.

[21] Dramatically improve your commute: convenient carpools with co-workers and neighbors. https://www.takescoop.com/; 2019.

[22] Arroyo JM. Bilevel programming applied to power system vulnerability analysis under multiple contingencies, IET generation. Transm Distrib 2010;4(2):178–90.

[23] Harris E, F. Mathematics for physical science and engineering–symbolic computing applications in maple and mathematica. Elsevier; 2014.

[24] IBM CPLEX optimizer. https://www.ibm.com/analytics/cplex-optimizer; 2020. 30.

[25] Gurobi Optimization. https://www.gurobi.com/products/gurobi-optimizer; 2020. 30.

[26] Meng Q, Yang H. Benefit distribution and equity in road network design. Transp Res Part B Methodol 2002;36(1):19–35.

[27] Tesla claims. 'quickest production car in the world' title with new 100 kwh battery pack: 0-60 in 2.5s and 315 mile range. https://electrek.co/2016/08/23/tesla-100-kwh-battery-pack-quickest-car-ever/; 2019.

[28] The resultant time and energy consumption, https://github.com/jfct001/CarSharing/blob/master/Car_Sharing_Appendix.pdf, Accessed: 2020-05-03.

[29] Bozorg-Haddad O, Solgi M, Loáiciga A, H. Meta-heuristic and evolutionary algorithms for engineering optimization. John Wiley & Sons; 2017.